CHINESE JOURNAL OF MECHANICAL ENGINEERING
Vol. 23, No. 3, 2010

DOI: 10.3901/CJME.2010.03.***, available online at www.cjmenet.com; www.cjmenet.com.cn

Crystallographic Characteristic of Intermetallic Compounds in Al-Si-Mg Casting Alloys by Using Electron Backscatter Diffraction

ZOU Yongzhi[1], XU Zhengbing[1, 2], HE Juan[1], and ZENG Jianmin[1, 2, *]

1 *State Key Laboratory of Solidification Processing, Northwestern Polytechnical University, Xi'an 710072, China*
2 *Key Laboratory of Nonferrous Materials and New Processing Technology of Ministry of Education, Guangxi University, Nanning 530004, China*

Received February 8, 2009; revised April 22, 2010; accepted April 30, 2010; published electronically May 10, 2010

Abstract: The Al-Si-Mg alloy which can be strengthened by heat treatment is widely applied to the key components of aerospace and aeronautics. Iron-rich intermetallic compounds are well known to be strongly influential on mechanical properties in Al-Si-Mg alloys. But intermetallic compounds in cast Al-Si-Mg alloy intermetallics are often misidentified in previous metallurgical studys. It was described as many different compounds, such as AlFeSi, Al_8Fe_2Si, $Al_5(Fe,Mn)_3Si_2$ and so on. For the purpose of solving this problem, the intermetallic compounds in cast Al-Si alloys containing 0.5% Mg were investigated in this study. The iron-rich compounds in Al-Si-Mg casting alloys were characterized by optical microscope (OM), scanning electron microscope (SEM), energy dispersive X-ray spectrometer (EDS), electron backscatter diffraction (EBSD) and X-ray powder diffraction (XRD). The electron backscatter diffraction patterns were used to assess the crystallographic characteristics of intermetallic compounds. The compound which contains Fe/Mg-rich particles with coarse morphologies was $Al_8FeMg_3Si_6$ in the alloy by using EBSD. The compound belongs to hexagonal system, space group $P\bar{6}2m$, with the lattice parameter a=0.662 nm, c=0.792 nm. The β-phase is indexed as tetragonal Al_3FeSi_2, space group I4/mcm, a=0.607 nm and c=0.950 nm. The XRD data indicate that $Al_8FeMg_3Si_6$ and Al_3FeSi_2 are present in the microstructure of Al-7Si-Mg alloy, which confirms the identification result of EBSD. The present study identified the iron-rich compound in Al-Si-Mg alloy, which provides a reliable method to identify the intermetallic compounds in short time in Al-Si-Mg alloy. Study results are helpful for identification of complex compounds in alloys.

Key words: Al-Si-Mg alloys, intermetallic compound, electron backscatter diffraction (EBSD), X-ray powder diffraction (XRD)

1 Introduction

Some of the most important industrial aluminum casting alloys are found in the Al-Si system. The addition of Mg makes the Al-Si alloy heat treatable. The Al-7Si-Mg alloy which can be strengthened by heat treatment is widely applied to the key components of aerospace and aeronautics mainly due to the combination of high strength and excellent casting properties[1–5]. However, some mechanical properties of the Al-7Si-Mg cast alloy, in particular, ductility, toughness, corrosion resistance and fatigue resistance, are affected by the morphology and distribution of the second phases.

Some of the iron-rich intermetallic compounds are associated with reduced mechanical properties. For example, the elongation of the Al-7Si-Mg casting alloy reduced from 7.0 to 3.0% as the content of iron increased from 0.17 to 0.60%[6].

Moreover, the Al-7Si-Mg alloy is a heat treatable alloy because magnesium is added to induce age hardening through precipitation of Mg-Si particles during heat processing[7]. But the melting point of iron-rich intermetallic compounds is lower than the eutectic temperature of the Al-7Si-Mg alloy，which will cause overburning during heat treatment[8] and reduce the mechanical properties distinctly. So the iron-rich intermetallic compounds are detrimental to mechanical properties of the Al-7Si-Mg alloy. It would be of great siginificance to accurately identify the iron-rich intermetallic compounds in the Al-7Si-Mg alloy.

Morphology, X-ray diffraction (XRD), convergent beam electron diffraction (CBED) and transmission electron microscope (TEM) have been used to identify the iron-rich intermetallic compounds. Eectron backscatter diffraction (EBSD) /scanning electron microscope (SEM) analysis have many vantages of the optical microscope (OM) and the TEM[9, 10]. It can provide an overall indication of the iron-rich intermetallic compounds and show the crystallographic orientation that is important for explicit identification of the iron-rich intermetallic compounds in alloys[11].

* Corresponding author. E-mail: zjmg@gxu.edu.cn
This project is supported by National Natural Science Foundation of China (Grant No.50864002), and Guangxi Provincial Natural Science Foundation of China (Grant No.0991001)

The coarse iron-rich compounds were described as many different compounds in previous studys[8, 10, 12–14]. It is clear that there is a poor understanding of the coarse iron-rich intermetallic compounds in Al-7Si-Mg casting alloys, even though the intermetallic compounds have a pronounced influence on properties. Therefore, accurate identification of the coarse iron-rich compounds in Al-7Si-Mg casting alloys is important because of the disagreement on the indentificaion of the intermetallic compounds.

In previous study, EBSD was applied to determine the eutectic Al-Si phase formation mechanism, through comparing the orientation of the aluminum in the eutectic to the orientation of the surrounding primary aluminum dendrites using automated crystal orientation mapping[15–18].

EBSD is also a useful technique for the identification of a micro-size phases because the electron backscattering patterns can be obtained from the individual particles. Exploiting the excellent imaging capability, EBSD can provide identification of unknown crystalline phases. In present study, the different iron-rich intermetallic compounds in Al-7Si-Mg casting alloy were observed and identified by SEM/EBSD.

2 EBSD and XRD experiment

2.1 Preparation of experimental material

The initial target chemical composition after all additions of the Al-7Si-Mg alloy is given in Table 1. The alloy was melted in an electric resistance furnace and the temperature of the melt was kept at 730 °C. Prior to pouring, the molten metal was degassed using C_2Cl_6 for 15 min to reduce the hydrogen content. The melt was poured at about 720 °C into a sand mould.

Table 1. Chemical composition and mass fraction of Al-7Si-0.5Mg alloy

Alloy Element	Si	Mg	Fe	Ti	Mn	Cu	Al
Mass fraction *w*/%	7.1	0.5	0.08	0.18	<0.01	<0.01	Bal.

2.2 Sample preparation for EBSD/SEM analysis

Then the metallographic specimens were prepared for EBSD/SEM analysis. In this study, specimens were 10 mm×10 mm×3 mm and mounted in the bakelite. Sample preparation is the key factor to obtain good quality EBSD patterns since EBSD is very sensitive to surface condition. The diffraction pattern signal comes from the top few nanometer, and any residual surface deformation introduced during the preparation must be minimized [19].

2.3 Identification of the intermetallic compounds by EBSD/SEM analysis

The samples were analyzed by OM, a HITACHI S-3400 SEM equipped with a GENESIS energy dispersive X-ray diffraction detector system (EDS) device, and EDAX TSL OIM EBSD system. In this study, the sample stage was pre-tilted 70° required for EBSD pattern acquisition and the acceleration voltage of SEM was 25 kV.

A general identification procedure carried out by EBSD/SEM can obtain a SEM image and EDS spectrum of an interesting particle, and then tilt to the 70° orientation required for EBSD pattern acquisition with keeping the same particle in view field during the tilting. The EBSD patterns of more than 30 different points of the interesting coarse and plate-like particles in the alloy were obtained and identified respectively.

2.4 XRD experiment

The compound and structural characterization of the Al-7Si-Mg alloy were obtained by X-ray powder diffraction (powder diffraction) of 40 kV Cu Kα radiation (Rigaku D/MAX 2500V). The XRD scan range was from 20º to 90º with a step size of 0.02º.

3 Results and Discussion

3.1 Metallographic analysis

Optical micrograph of the alloy is shown in Fig. 1. A coarse lamellar eutectic silicon structure is observed. The fishbone-like Mg_2Si phase, bulky π-phase and plate-like β-phase are observed in Fig. 1(b). The coarse π-phase particles are found at primary aluminum dendrite boundaries. And some plate shaped β-phase particles exist along eutectic colony boundaries.

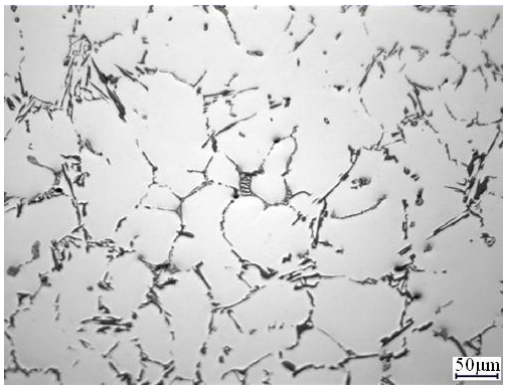

(a) Low magnitude image

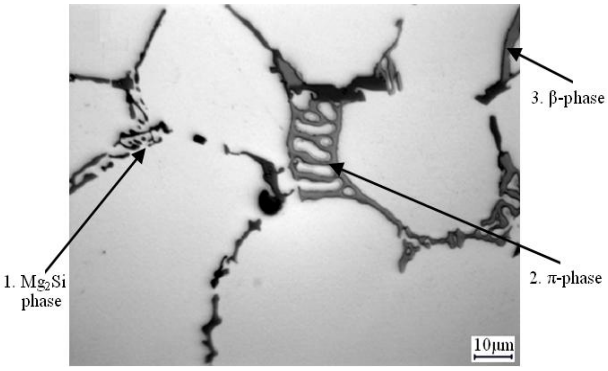

(b) Centric area of Fig. 1(a) with higher magnitude

Fig. 1. Morphology of the Al-7Si-Mg samples

3.2 EBSD analysis

In ordr to identifing the intermetallic compounds, there are three things to be done. Firstly a SEM image of an interesting particle was obtained. Secondly EDS analysis to confirm the phase was performed. Finally the EBSD pattern was acquired and analysed.

The locations of iron-intermetallic particles within the samples can be determined easily by morphology observation as well as the EDS analysis results. The SEM image and X-ray mapping of the microstructure intermetallic compounds in the alloy are shown in Fig. 2. EDS analysis of the bulky π-phase particle revealed the presence of iron, manganese, aluminum and silicon, and the plate shaped β-phase exhibited the aluminum, silicon and iron characteristic peaks.

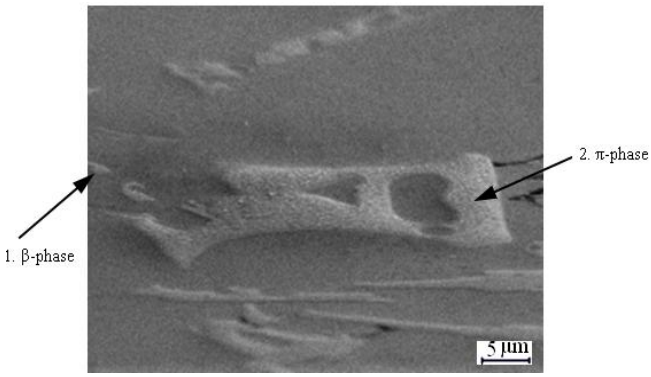

(a) SEM

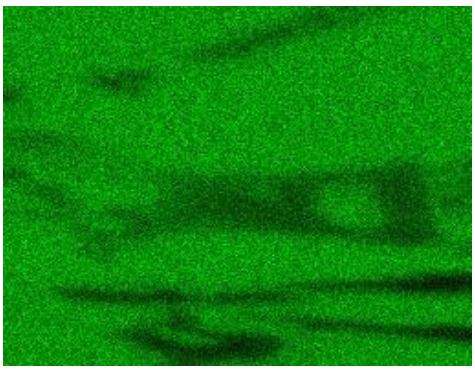

(b) Al

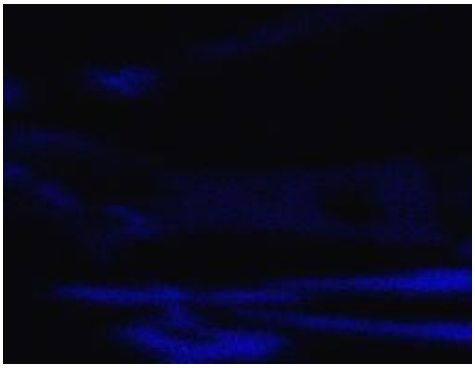

(c) Si

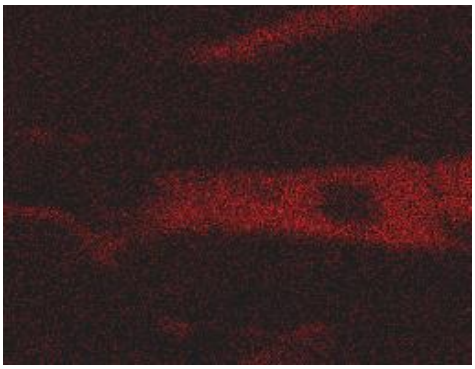

(d) Mg

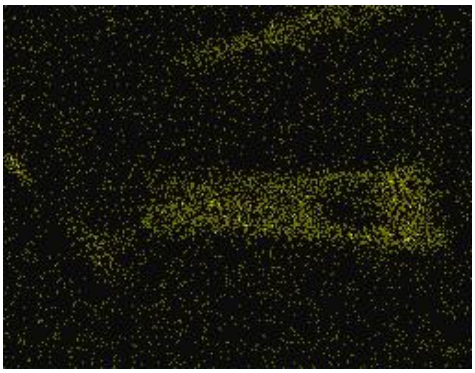

(e) Fe

Fig. 2. SEM image and EDS mapping of the π-phases

The EBSD is an appurtenance of SEM technique allowing the crystallographic orientation to be determined locally in the point where the electron beam is positioned. The EBSD was indexed by software and the orientation dates were stored on a computer. The crystallographic data (atomic positions, space group, etc.) of intermetallic compounds were listed in Pearson's Handbook containing Al-Si, Al-Mg, Al-Si-Fe and Al-Si-Fe- Mg as possible phases. Before indexing a specific phase, the crystallographic data were adopted in the TSL OIM Data Collection 5.0 software databases. The simulation of the phase and a preliminary indexing of the Kikuchi patterns were performed through the data.

EBSD patterns contain a large amount of information

about the crystal structure of the phase. The information can determine the space group of the phase from the symmetry elements contained in the pattern. EBSD patterns also contain higher order Laue zone rings (HOLZ) which have been used to accurately measure lattice plane spacing and have also been used to determine the reduced unit cell of the phase[19].

Contrary to the results of previous study on similar intermetallics[8,10], each of these representative experimental EBSD patterns was found to be consistent with hexagonal $Al_8FeMg_3Si_6$, with space group $P\bar{6}2m$ and lattice parameter a=0.662 nm, c=0.792 nm. Fig. 3 is the EBSD/EDS/SEM study of the π-phase indexed as $Al_8FeMg_3Si_6$ with EDAX-TSL in the alloy. Firstly the morphology of coarse π-phase particle was obtained by SEM (Fig. 3(a)), and EDS spectrum for π-phase particle is shown in Fig. 3(b). Then the representative experimental EBSD pattern of the π-phase was gained by using EBSD (Fig. 3(c)). Fig. 3(d) and Fig. 3(e) illustrate the identification of Kikuchi lines, and Fig. 3(f) is the identification of the Kikuchi line pairs. Fig. 3(g) and Fig. 3h show the EBSD pattern and the crystal structure of the π-phase with TSL-OIM simulations under the same orientation.

In previous study, the plate-shaped phase was also identified as many different compounds. In this present study, EBSD patterns of the β-phase are consistent with tetragonal Al_3FeSi_2, space group I4/mcm, a=0.607 nm and c=0.950 nm though the EBSD patterns of β-phase that is not depicted. And the β-phase was also investigated by XRD to confirm the results.

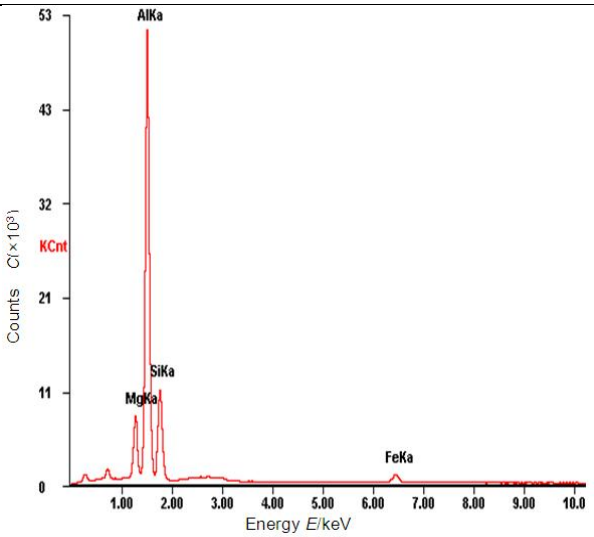

(b) EDS spectrum

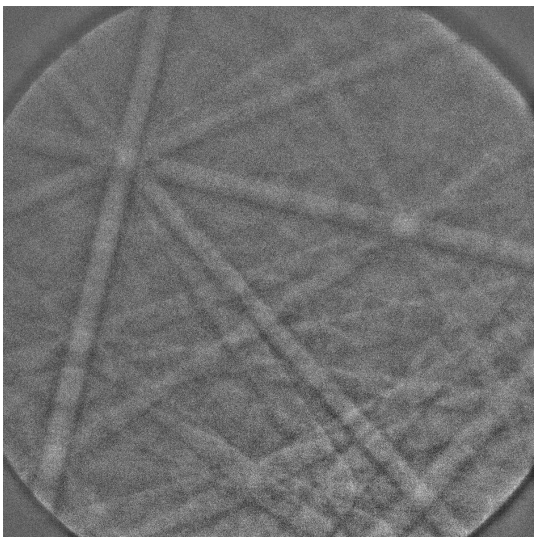

(c) Representative experimental EBSD pattern

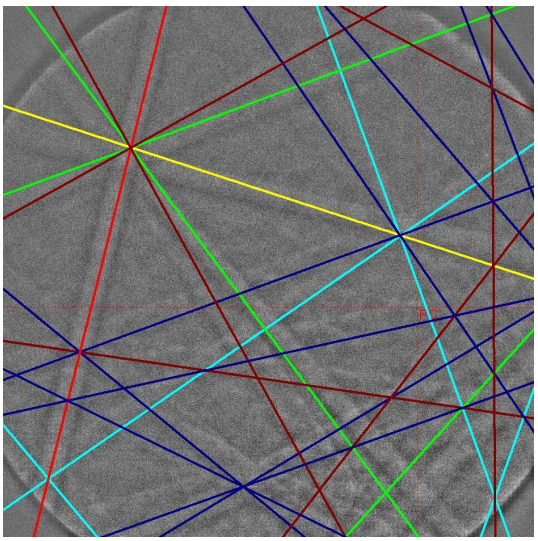

(d) Identification of Kikuchi lines

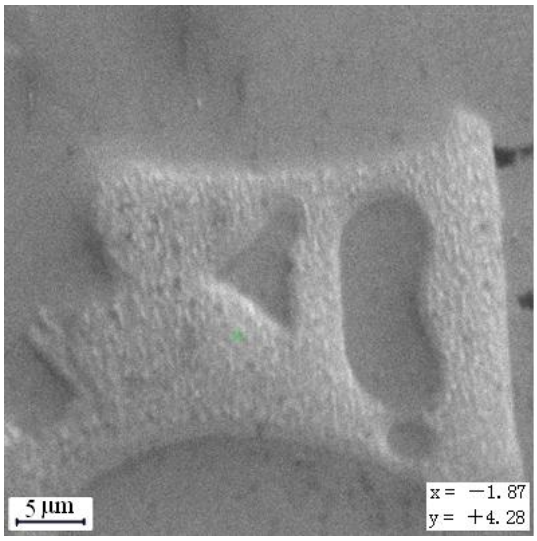

(a) SEM image

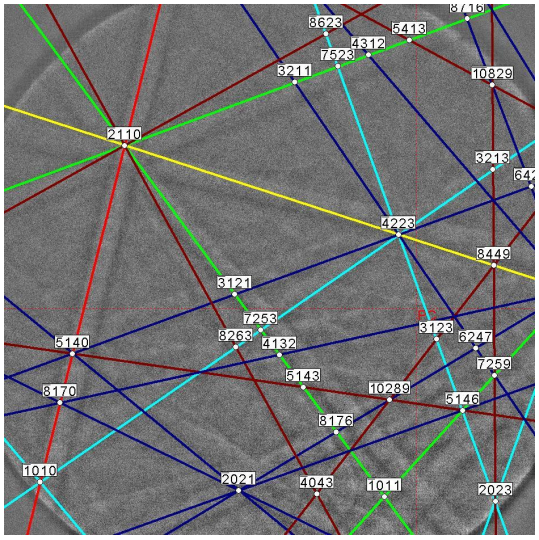

(e) Identification of Kikuchi lines

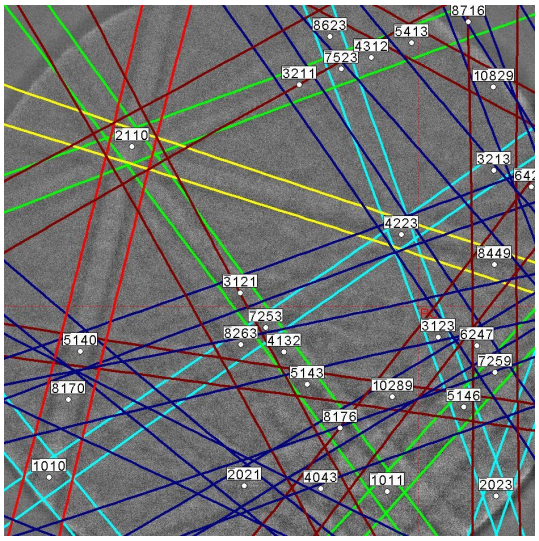

(f) Identification of the Kikuchi line pairs

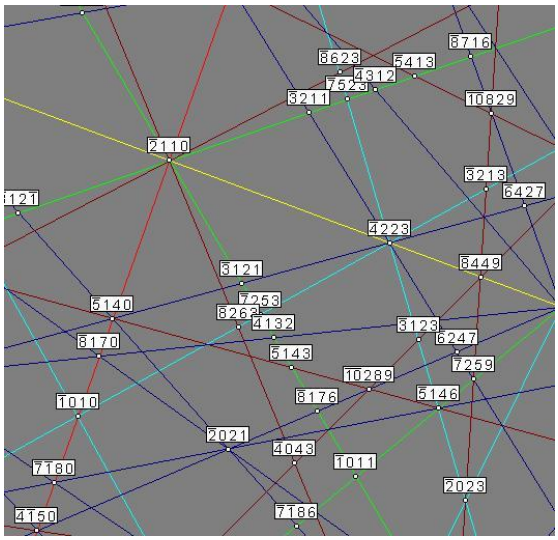

(g) EBSD pattern of π-phase with TSL-OIM simulations

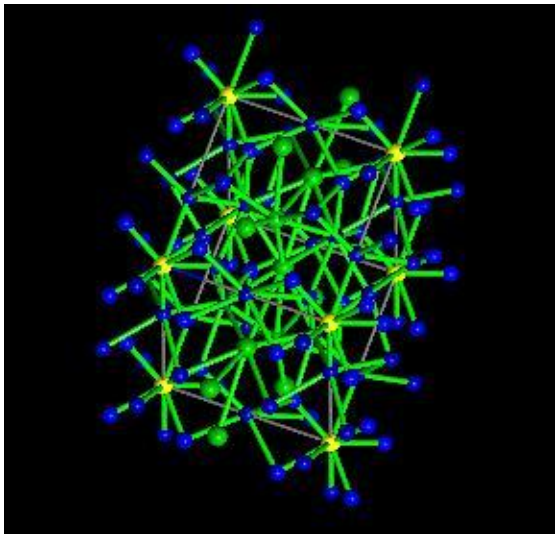

(h) Crystal structure of π-phase with TSL-OIM simulations

Fig. 3. EBSD/EDS/SEM study of the π-phase indexed as $Al_8FeMg_3Si_6$ with EDAX-TSL simulations

3.3 XRD analysis

The calculated intensity y_{ci} are determined by summing the contributions from neighboring Bragg reflections for all phases, plus the background. The modified formula of the Rietveld method is expressed as

$$y_{ci} = S_r \left\{ \sum_p S_p A_b \left\{ S_K \left[|F_s|^2 \varphi(2\theta_i - 2\theta_H) \; A_s L_f P_f \right] \right\}_P + y_{bi} \right\}, \tag{1}$$

where y_{ci}—Calculated intensity,
S_p—Scale factor for phase P,
S_r—Function to model the effects of surface roughness,
A_b—Absorption factor,
F_s—Structure factor,
φ—Reflection profile function,
L_f—Lorentz, polarization and multiplicity factors,
P_f—Preferred orientation function,
y_{bi}—Background intensity.

From Eq. (1), the weight fraction for each phase is related to the scale factor S_P. Therefore, the weight fraction for each phase can be calculated by using the relation of weight fraction and scale factor.

The program calculates weight fraction for each phase refined, on the assumption that phases refined account for 100% of the specimen, via the following relation:

$$W_p = \frac{S_p (MV)_p}{\sum_{i=1}^{n} S_i (MV)_i}, \tag{2}$$

where p—Value of i for a particular phase in n phases,

S_i—Refined scale factor,

M—Weight of the unit cell in atomic weight units,

V—Volume of the unit cell.

In this study, the R_{wp} factor is used to verify the Rietveld method:

$$R_{wp}=\left[\frac{\sum_i W_i\left(y_{ei}-y_{ci}\right)^2}{\sum_i W_i\left(y_{ei}\right)^2}\right]^{1/2}, \quad (3)$$

where y_{ei}—Experimental intensity of $2\theta_i$,

y_{ci}—Calculated intensity of $2\theta_i$,

W_i—Weight factor.

In an ordinary condition, the refinement result is considered to be reliable when R_{wp} reachs about 10%.

The Rietveld refinement of phases was performed by using the DBWS9807 program[20]. The Pseudo-Voigt function was used for the simulation of the peak shapes. The DMPLOT view program[21] was used to follow the refinement results. The indexed results were used as the starting lattice parameters. A total of 41 parameters were refined, including scale factor, coefficients for the polynomial function describing the angular variation of the background (5 parameters), lattice parameters, full width at half maximum, preferred orientation, atomic coordinates, site occupancy and so on were refined.

The X-ray powder diffraction diagram after refinement of the alloy is shown in Fig. 4. By using quantitative XRD, the volume fraction results are listed in Table 2. XRD data indicate that $Al_8FeMg_3Si_6$ and Al_3FeSi_2 are present in the microstructure of Al-7Si-Mg alloy.

All reflections of the π-phase are adequately indexed as hexagonal $Al_8FeMg_3Si_6$, space group $P\bar{6}2m$, with the lattice parameters a=0.662 nm, c=0.792 nm, and the R_{wp} is 7.17%. The β-phase was indexed as tetragonal Al_3FeSi_2, with space group I4/mcm, a=0.607 nm and c=0.950 nm. And the R_{wp} is 7.29%.

The structures of iron-rich compounds have been determined to comfort the results of EBSD/SEM by Rietveld refinement of X-ray powder diffraction data.

Table 2. Volume fraction of phases in the test alloy

Phase	Al	Si	Mg_2Si	$Al_8FeMg_3Si_6$	Al_3FeSi_2
Volume fraction v/%	92.93	6.18	0.64	0.14	0.11

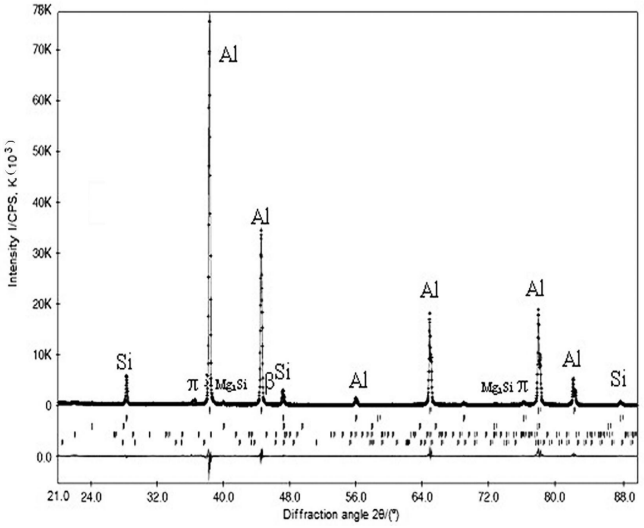

Fig. 4. Results of the Rietveld method: Experimental (dot) and calculated (continuous curve) patterns of the sample

The difference profile is shown at the bottom of the Fig.4: vertical markers at the bottom indicate the position of the calculated Bragg reflections.

3.4 Discussion

The Fe element can not be found by EDS in the Al dendrites of the alloy. Almost all the iron, therefore, is incorporated into the intermetallic compounds, because the iron saturability of Al solution is low, only 0.05%.

Identification of iron-rich intermetallic compounds by their morphology is inaccurate because the morphology of iron compound in Al-Si alloys is various. Also, EDS and XRD results are not su cient for identification of phases. Therefore, most of the studies claiming to have identified iron-rich intermetallic particles as some specific compound solely by morphology and/or semi-quantitative compositional analysis were partially incorrect at least. In previous study, the intermetallic compounds have been described as many different compounds, such as AlFeSi[12], Al_8Fe_2Si, $Al_5(Fe,Mn)_3Si_2$[8] and so on. The morphology of iron compound can be improved by melt superheating, increasing cooling-rate, adding trace elements and so on. In the recent KRAL's work[13, 14], the bulky compound is consistent with cubic $Al_9(Mn,Fe)_5Si_2$ designated as by SEM/EBSD and TEM/CBED because they added Mn into Al-Si alloys in order to change needle-like iron compound into Chinese scripts or other better shapes.

In present study, the different iron-rich intermetallic compounds in Al-7Si-Mg casting alloy were observed and identified by SEM/EBSD. The X-ray powder diffraction (XRD) experiment confirmed the EBSD results. The combination with SEM, EDS and EBSD provides a reliable method to identify the intermetallic compounds in short time.

4 Conclusions

(1) The crystal structures of iron-rich intermetallics commonly designated as π-phase and β-phase were

obtained with SEM via EBSD and affirmed by XRD experiment.

(2) The π-phase is adequately described as hexagonal $Al_8FeMg_3Si_6$, space group $P\bar{6}2m$, with lattice parameter a=0.662 nm, c=0.792 nm.

(3) The β-phase is indexed as tetragonal Al_3FeSi_2, space group I4/mcm, a=0.607 nm and c=0.950 nm.

(4) The XRD data indicate that $Al_8FeMg_3Si_6$ and Al_3FeSi_2 are present in the microstructure of Al-7Si-Mg alloy, which confirms the identification result of EBSD.

(5) EBSD in the SEM provides a reliable method to identify the intermetallic compounds in short time.

References

[1] DAHLE A K, NOGITA K, MCDONALD S D, et al. Eutectic modification and microstructure development in Al-Si Alloys[J]. *Materials Science and Engineering A*, 2005, 413–414(12): 243–248.

[2] THIRUGNANAM A, SUKUMARAN K, PILLAI U T S, et al. Effect of Mg on the fracture characteristics of cast Al-7Si-Mg alloys[J]. *Materials Science and Engineering A*, 2007, 445–446(2): 405–414.

[3] KLIAUGA A M, VIEIRA E A, FERRANTE M. The influence of impurity level and tin addition on the ageing heat treatment of the 356 class alloy[J]. *Materials Science and Engineering A*, 2008, 480(3): 5–16.

[4] LIU XiangFa, QIAO JinGuo, WU YuYing, et al. EPMA analysis of calcium-rich compounds in near eutectic Al-Si alloys[J]. *Journal of Alloys and Compounds*, 2005, 388 (2): 83–90.

[5] SHABESTARI S G, MOEMENI H. Effect of copper and solidification conditions on the microstructure and mechanical properties of Al-Si-Mg alloys[J]. *Journal of Materials Processing Technology*, 2004, 153–154(11): 193–198.

[6] MURALI S, RAMAN K S, MURTHY K S S. Morphological studies on β-FeSiAl5 phase in Al-7-Si-0.3Mg alloy with trace additions of Be, Mn, Cr, and Co[J]. *Materials Characterization*, 1994, 33(9): 99–112.

[7] ROMETSCH P A, SCHAFFER G B. An age hardening model for Al-7Si-Mg casting alloys[J]. *Materials Science and Engineering A*, 2002, 325(1–2): 424–434.

[8] MONDOLFO L F. *Aluminum alloys: structure and properties*[M]. London/Boston: Butterworth & Co (Publishers) Ltd, 1976.

[9] WANG Q G, APELIAN D, ARNBERG L, et al. Solidifacation of the eutectic in hypoeutectic Al-Si alloys[J]. *AFS Transactions*, 1999, 107: 249–256.

[10] HUMPHREYS F J. Quantitative metallography by electron backscattered diffraction[J]. *Journal of Microscope*, 1995, 195(3): 170–185.

[11] NOGITA K, DAHLE A K. Eutectic solidification in hypoeutectic Al–Si alloys: electron backscatter diffraction analysis[J]. *Materials Characterization*, 2001, 46(4): 305–310.

[12] REDFORD K, TIBBALLS J E, McPHERSON R. Calorimetric data for α-AlMnSi and the α-to-β decomposition [J]. *Thermochimica Acta*, 1990, 158(1): 115–123.

[13] KRAL M V. A crystallographic identification of intermetallic phases in Al-Si alloys[J]. *Materials Letters*, 2005, 59(18): 2271–2276.

[14] KRAL M V, MCINTYRE H R, SMILLIE M J. Identification of intermetallic phases in a eutectic Al–Si casting alloy using electron backscatter diffraction pattern analysis[J]. *Scripta Materialia*, 2004, 51(3): 215–219.

[15] NOGITA K, KNUUTINEN A, MCDONALD S D, et al. Mechanisms of eutectic solidification in Al–Si alloys modified with Ba, Ca, Y and Yb[J]. *Journal of Light Metals*, 2001, 1(4): 219–228.

[16] DAHLE A K, NOGITA K, ZINDEL J W, et al. Eutectic nucleation and growth in hypoeutectic Al-Si alloys at different strontium levels[J]. *Metallurgical and Materials Transaction A*, 2001, 32(4): 949–960.

[17] HEIBERG G, NOGITA K, DAHLE A K, et al. Columnar to equiaxed transition of eutectic in hypoeutectic aluminum–silicon alloys[J]. *Acta Materialia*, 2002, 50(10): 2 537–2 546.

[18] HEIBERG G, NOGITA K. Investigation of the microstructure of the Al-Si eutectic in binary aluminium-7wt% silicon alloys by electron backscatter diffraction (EBSD)[J]. *Journal of Light Metals*, 2001, 1(1): 43–49.

[19] SCHWARTZ A J, KUMAR M, BRENT L A. *Electron backscatter diffraction in materials science*[M]. New York: Kluwer Academic/ Plenum Publishers, 2001.

[20] YONG R A, SAKTHIVEL A, MOSS T S, et al. DBWS-9411- an upgrade of DBWS*.* programs for Rietveld refinement with PC and mainframe computers[J]. *Journal of Applied Crystallography*, 1995, 28(3): 366–367.

[21] MARCINIAK H, DIDUSZKO R. *DMPLOT-Plot view program for rietveld refinement method*[M]. Version 3.38. Warsaw: High Pressure Research Centre UNIPRESS, 1997.

Biographical notes

ZOU Yongzhi, born in 1978, is a PhD candidate on material science and technology in State Key Laboratroy of Solidification Processing, Northwestern Polytechnical University, China. She received her master degree on materials physical and chemistry, Guangxi University, China, in 2004. Her study focuses on nonferrous materials.
Tel: +86-771-3231238; E-mail: zyz2007@126.com

XU Zhengbing, born in 1979, is a PhD candidate on material science and technology in State Key Laboratroy of Solidification Processing, Northwestern Polytechnical University, China. He received his master degree on materials physical and chemistry, Guangxi University, China, in 2004. His study focuses on nonferrous materials.
Tel: +86-771-3231238; E-mail: 51happiness@163.com

HE Juan, born in 1983, is a PhD candidate on material science and technology in State Key Laboratroy of Solidification Processing, Northwestern Polytechnical University, China. She received her master degree on materials physical and chemistry, Guangxi University, China, in 2008. Her study focuses on nonferrous materials.
Tel: +86-771-3231238; E-mail: shanxihj@163.com

ZENG Jianmin, born in 1955, is a professor in Guangxi University. He received his PhD degree from State Key Laboratroy of Solidification Processing, Northwestern Polytechnical University, China, in 1991. His study interests include nonferrous materials and processing, nonferrous casting, etc.
Tel: +86-771-3231238; E-mail: zjmg@gxu.edu.cn